Cell Reports, Volume *23*

Supplemental Information

Shp-2 Is Dispensable for Establishing T Cell Exhaustion and for PD-1 Signaling *In Vivo*

Giorgia Rota, Charlène Niogret, Anh Thu Dang, Cristina Ramon Barros, Nicolas Pierre Fonta, Francesca Alfei, Leonor Morgado, Dietmar Zehn, Walter Birchmeier, Eric Vivier, and Greta Guarda

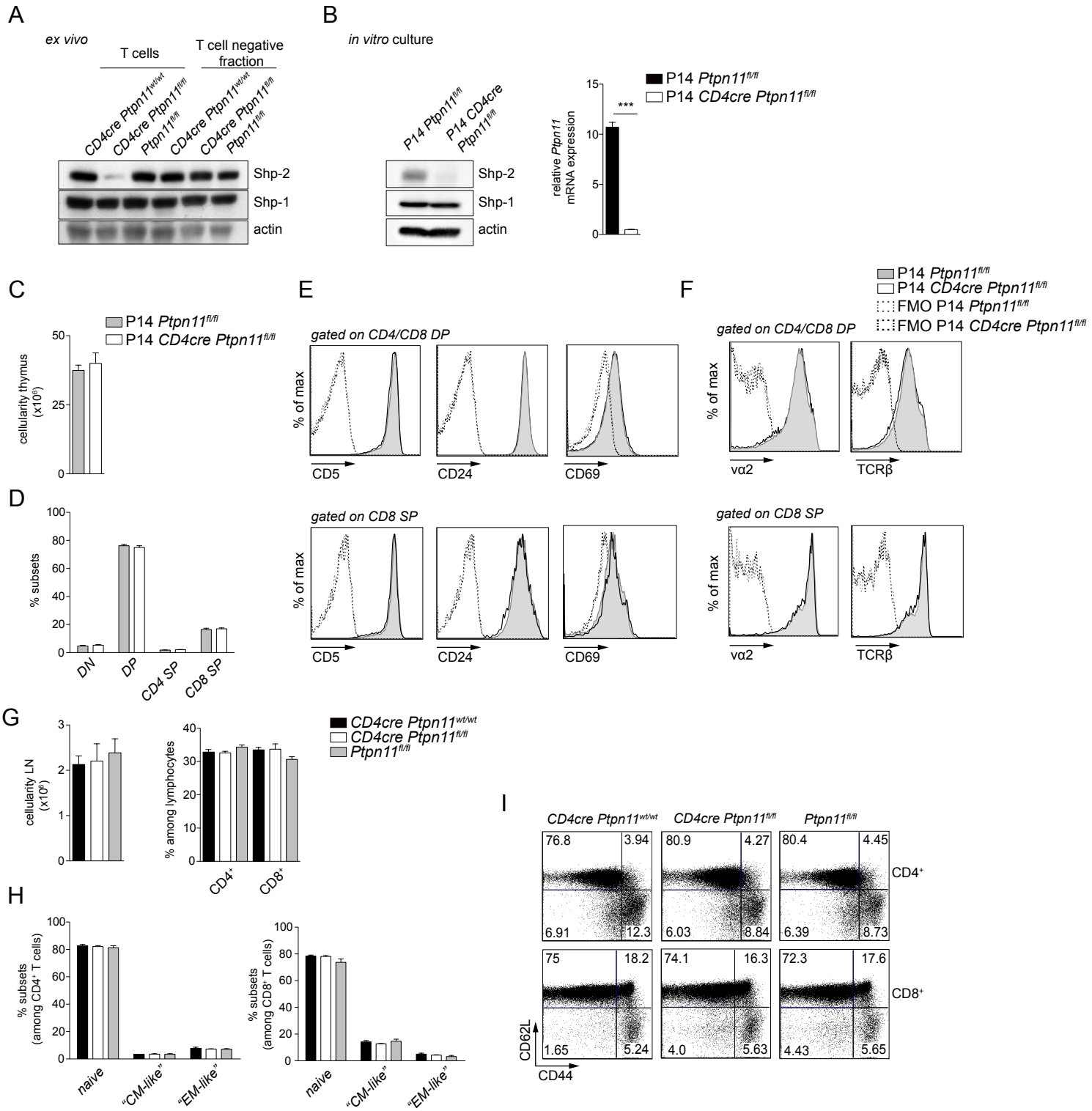

Figure S1. Shp-2 is deleted in T cells and *CD4cre Ptpn11$^{fl/fl}$* mice show normal T cell selection and peripheral homeostasis . Related to Figure 1. A) Total T cells were enriched from spleens of *CD4cre Ptpn11$^{wt/wt}$*, *CD4cre Ptpn11$^{fl/fl}$* and *Ptpn11$^{fl/fl}$* mice. The remaining fraction is indicated as T cell-negative. Expression of Shp-2 or Shp-1 was tested by immunoblot in cell lysates from the indicated subsets, actin used as loading control. T cell purity was over 90%, whereas T cell contamination in T cell-depleted spenocytes less than 5%. B) CD8$^+$ T cells were enriched from spleens of P14 transgenic *CD4cre Ptpn11$^{fl/fl}$* and *Ptpn11$^{fl/fl}$* mice, with a purity of over 97%. Cell were activated with plastic-bound α-CD3 and α-CD28 (1μg/ml each, in the presence of 10 ng/ml IL-2) for 48 hours and cultured for additional 48 hours (in the presence of 20 ng/ml IL-2). Cells were then collected and expression of Shp-2 or Shp-1 was tested by immunoblot (left panel) and abundance of *Ptpn11* mRNA determined by quantitative RT-PCR (relative to *Polr2a*; right panel). Quantitative RT-PCR data represent mean ± SD of n=3 technical replicates and are representative of at least two independent experiments. C-F) Analysis of thymi from P14-transgenic *CD4cre Ptpn11$^{fl/fl}$* and *Ptpn11$^{fl/fl}$* mice. C and D) Cellularity (C) and percentages of DN, DP, and SP thymocytes among lineage-negative lymphocytes (D) are depicted. E and F) A representative histogram illustrates the levels of CD5, CD24, and CD69 (E) and of Vα2 and TCRβ (F) on DP and CD8 SP. G) Inguinal lymph nodes (LNs) cellularity and percentages of CD4$^+$ (CD4$^+$ CD3$^+$) and CD8$^+$ (CD8$^+$ CD3$^+$) T cells (gated on lymphocytes) in *CD4cre Ptpn11$^{wt/wt}$*, *CD4cre Ptpn11$^{fl/fl}$*, and *Ptpn11$^{fl/fl}$* mice are illustrated. H and I) Percentages of naïve (CD44$^{low\text{-}int}$CD62L^{high}), "CM-like" (CD44^{high} CD62L^{high}), and "EM-like" (CD44^{high} CD62L^{low}) CD4$^+$ and CD8$^+$ T lymphocytes in the iLNs of the afore-mentioned mice (H) and a representative flow cytometry plot of CD62L and CD44 expression (I) are depicted. Results represent mean ± SEM of n=4 mice/ group (C and D) and of n=3-5 mice/group (G and H) and are representative of two (C-F) or at least two (G-I) independent experiments. Only statistically significant differences are shown (B-D, G and H); Student's t-test; ***p ≤ 0.001

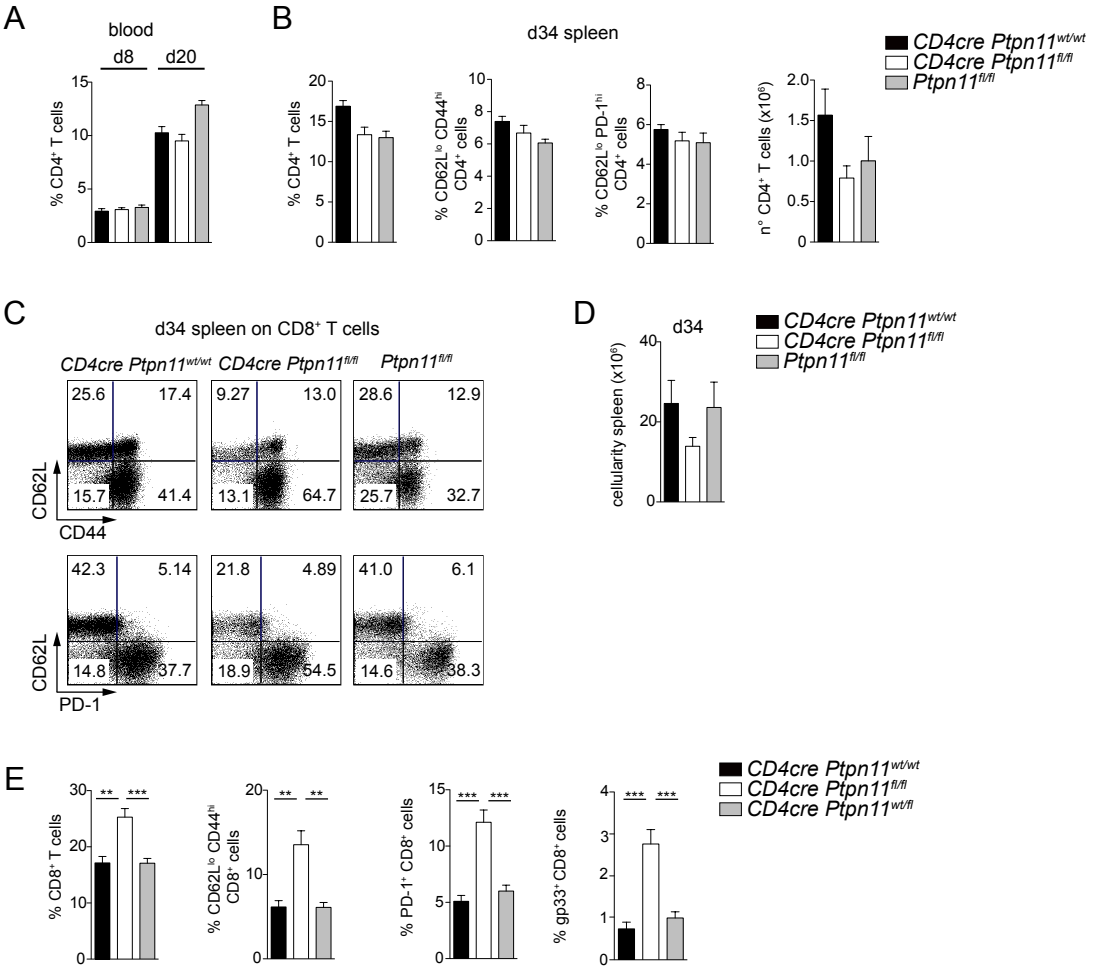

Figure S2. Characterization of T cells in *CD4cre Ptpn11$^{fl/fl}$* mice during chronic LCMV. Related to Figure 2
A) Graph illustrates percentages of CD4$^+$ T cells at day 8 and 20 p.i. in blood of *CD4cre Ptpn11$^{wt/wt}$*, *CD4cre Ptpn11$^{fl/fl}$* and *Ptpn11$^{fl/fl}$* mice. B) Graphs depict percentages and numbers of CD4$^+$ T cells, percentages of CD62L low CD44 high (CD62L^{lo} CD44^{hi}), and of CD62L low PD-1 high (CD62L^{lo} PD-1^{hi}) CD4$^+$ T cells at day 34 p.i. in the spleen of the afore-mentioned mice. C) Representative flow cytometry plots of CD62L/CD44 or CD62L/PD-1 expression on CD8$^+$ T cells at day 34 p.i. in the spleen. D) Graph shows spleen cellularity of *CD4cre Ptpn11$^{wt/wt}$*, *CD4cre Ptpn11$^{fl/fl}$* and *Ptpn11$^{fl/fl}$* mice at day 34 p.i.. E) Graphs illustrate percentages of CD8$^+$, CD44high CD62Llow effector, PD1$^+$, and gp33-specific (gp33$^+$) T cells among lymphocytes in the spleen of *CD4cre Ptpn11$^{wt/wt}$*, *CD4cre Ptpn11$^{fl/fl}$*, and *CD4cre Ptpn11$^{wt/fl}$* mice at day 34 p.i.. A, B, D, and E) Results are a pool of two independent experiments, and mean ± SEM of n=6-15 (A), n=6-12 (B and D), n=7-8 (E) mice/group. Only differences statistically significant in comparison to both controls are shown; **p ≤ 0.01, ***p ≤ 0.001; Student's t-test

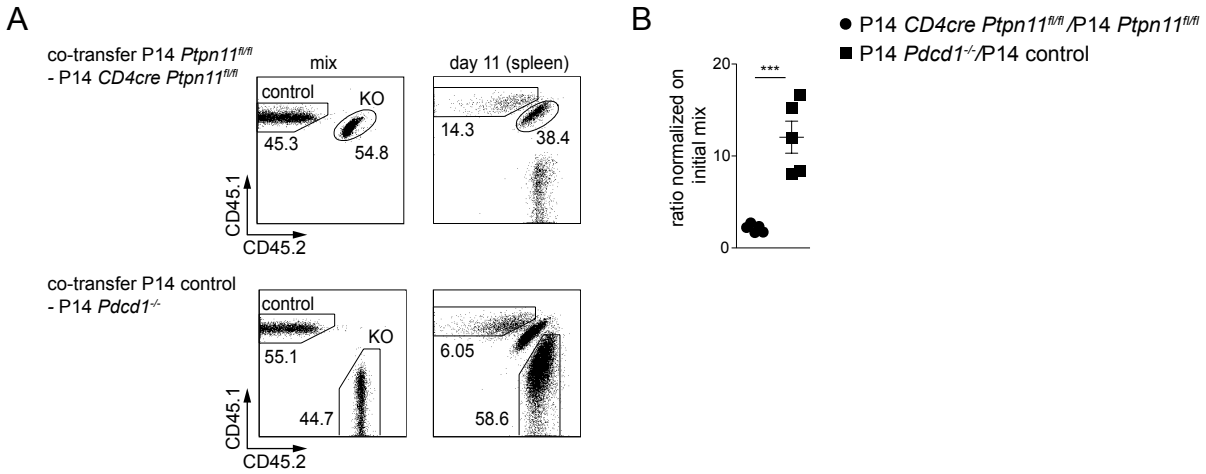

Figure S3. *Ptnp11*- and *Pdcd1*- deficient T cells show profound differences in expansion upon chronic LCMV. Related to Figure 3. Wild type recipient mice (CD45.2) were co-transferred with a mix of 400 control (*Ptpn11*$^{fl/fl}$, CD45.1) and 400 *Ptpn11*-deficient (KO; *CD4cre Ptpn11*$^{fl/fl}$, CD45.1/2) P14 CD8$^+$ T cells and infected with LCMV clone 13. In parallel, wild type mice (CD45.1/2) were co-transferred with a mix of 400 control (CD45.1) and 400 *Pdcd1*-deficient (KO; CD45.2) P14 CD8$^+$ T cells and infected with LCMV clone 13. A) Percentages of KO and control P14 T cells in the initial mix and in the spleen at day 11 p.i. are shown as a representative flow cytometry plot (gated on Va2$^+$ CD8$^+$ T cells). B) The graph depicts the ratio of *Ptpn11*- or *Pdcd1*- deficient over control (normalized to the initial mix) at day 11 in individual mice (n=5 mice/group); Only statistically significant differences are shown; ***$p \leq 0.001$; Student's t-test.

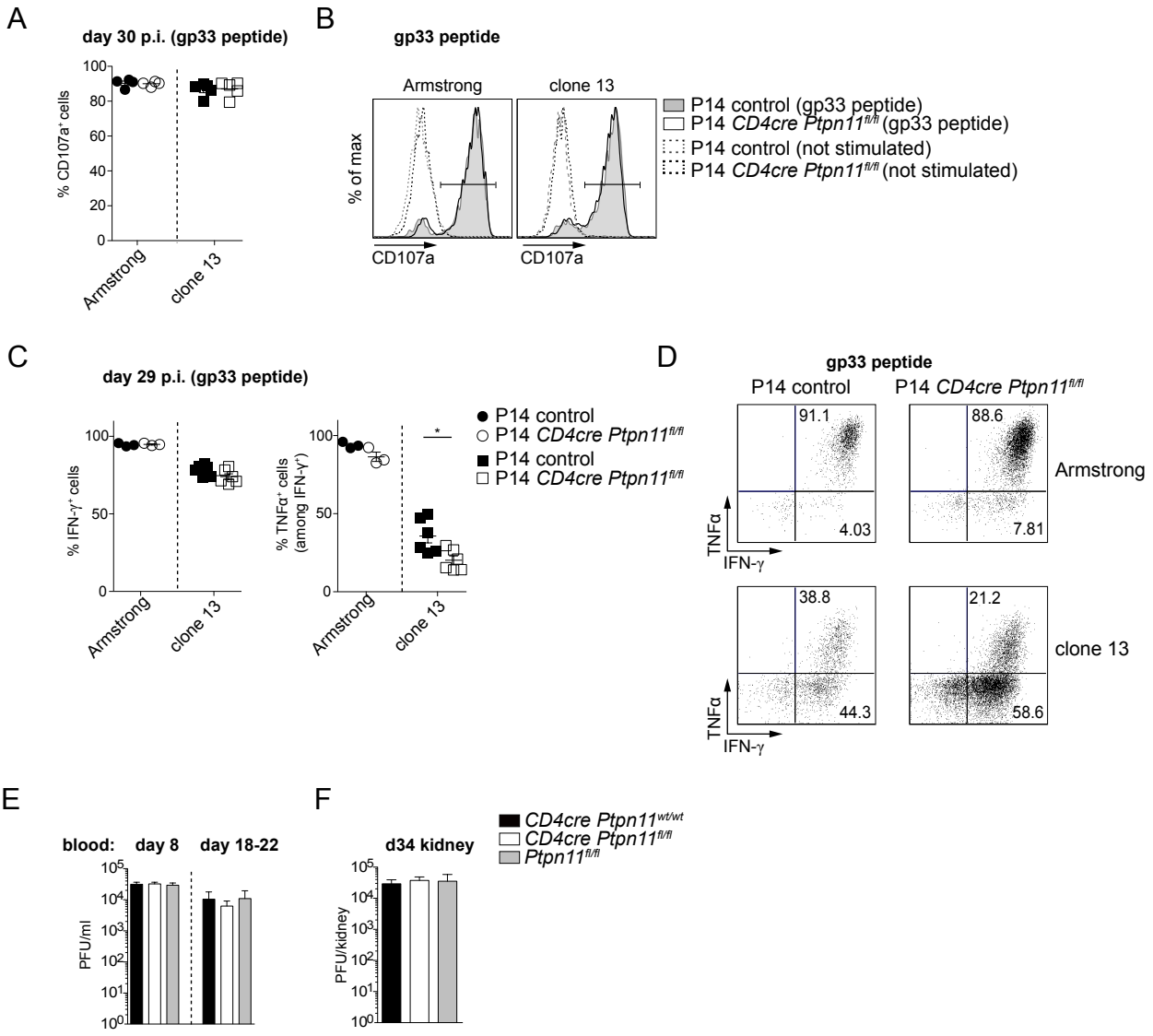

Figure S4. Functional characterization of *Ptnp11*-deficient T cells during chronic LCMV. Related to Figure 4
A-D) Wild type recipient mice were co-transferred with a 1:1 mix of congenically-marked control (*CD4cre Ptpn11*$^{wt/wt}$) and *Ptpn11*-deficient P14 CD8$^+$ T cells and infected with LCMV clone 13 or Armstrong, as a control. A-D) Splenocytes isolated at day 30 from infected mice were restimulated with gp-33 peptide pulsing and stained for CD107a (A and B), IFN-γ and TNF-α (C and D). Graphs (A, C) illustrate frequencies of CD107a$^+$ (A), IFN-γ$^+$, and TNFα$^+$ among IFN-γ$^+$ (C) *Ptpn11*-deficient and control P14 T cells, and representative flow cytometry pictures are shown (B, D). Results depict mean ± SEM of n=3-4 (Armstrong) and n=5-6 (clone 13) (A and C). Results confirm data shown in Figure 4B and C and were performed once with gp-33 restimulation (A and B) or are representative of at least two independent experiments (C and D). E and F) Viral titers at the indicated times in serum (E) and 34 days after infection with LCMV clone 13 in the kidney (F) from *CD4cre Ptpn11*$^{wt/wt}$, *CD4cre Ptpn11*$^{fl/fl}$ and *Ptpn11*$^{fl/fl}$ mice. Results illustrate mean ± SEM of n=4-9 mice/group (E) and n=6-12 mice/group (F) and are a pool of two independent experiments. Only statistically significant differences are shown; *p ≤ 0.05, Student's t-test.

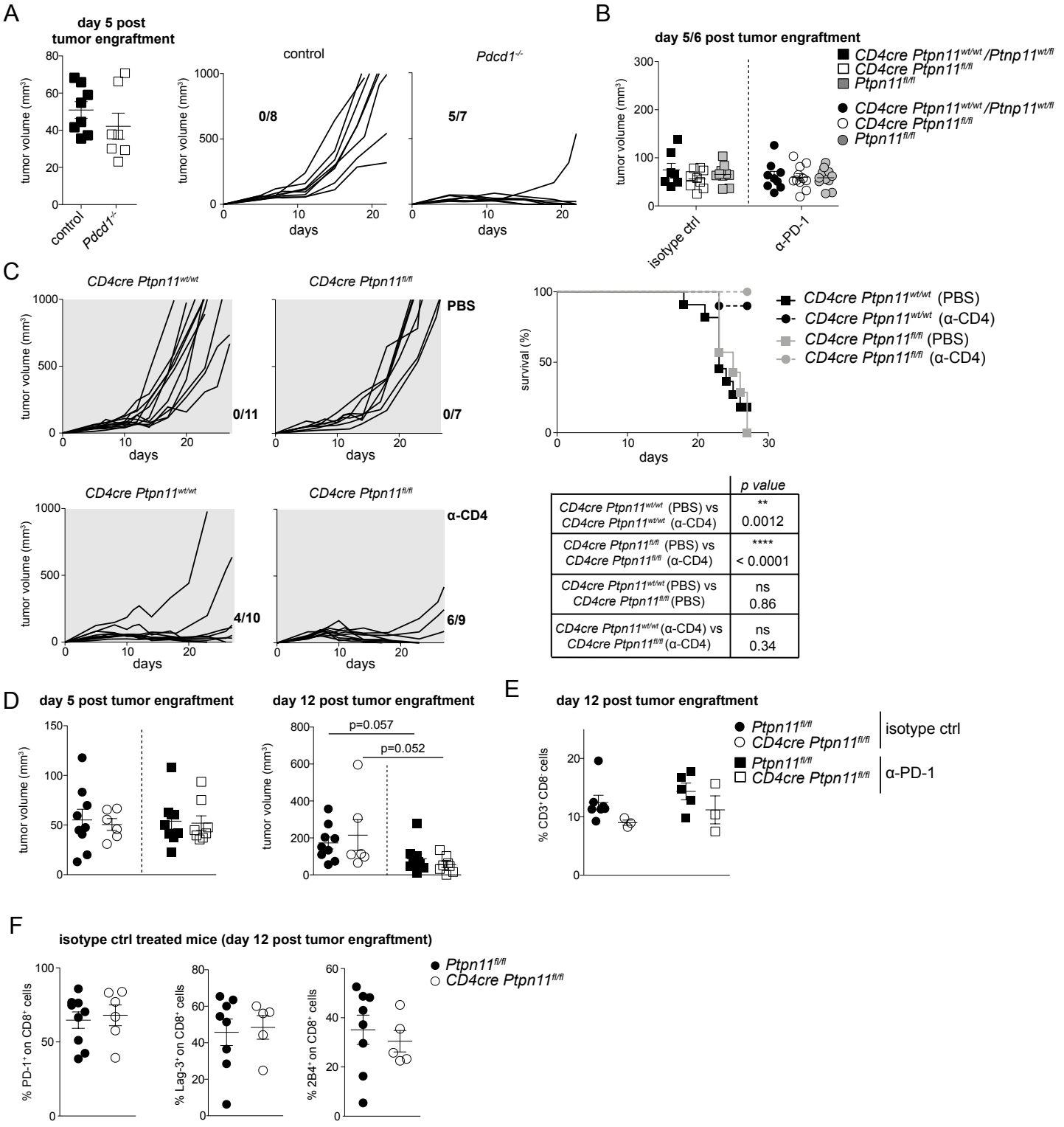

Figure S5. Control of MC38 engraftment in the absence of PD-1 signaling, helper T cells, and Shp2. Related to Figure 5.
A) Wild type and *Pdcd1*-deficient mice were subcutaneously inoculated with MC38 cells. Tumor growth in individual mice is shown at day 5 (*on the left*) and over time (*on the right*); the number of mice completely controlling tumor growth in each group is indicated within the graphs. B) Mice of the indicated genotypes were subcutaneously inoculated with MC38 cells. Graph depicts tumor volume 5-6 days after (depending on the experiment), when mice were randomized as indicated and treatment with α-PD1 antibody or isotype control was started. C) *CD4cre Ptpn11$^{wt/wt}$* and *CD4cre Ptpn11$^{fl/fl}$* mice were depleted of CD4$^+$ T cells by weekly i.p. injections of α-CD4-depleting antibody (GK1.5, BioXcell, 200 µg/mouse), or PBS as control, starting two days prior to MC38 engraftment. Tumor growth in individual mice is shown (*on the left*); the number of mice completely controlling tumor growth in each group is indicated next to the graphs. Survival curves and statistical comparisons are shown (*on the right*). D-F) *CD4cre Ptpn11$^{fl/fl}$* and *Ptpn11$^{fl/fl}$* mice were inoculated with MC38 cells. D) Graphs show tumor volume 5 days after inoculation (*on the left*), when mice were divided as indicated and treatment with α-PD-1 antibody or isotype control was started, and 12 days (*on the right*) after inoculation and three injections of α-PD1 antibody or isotype control. E) Graph depicts the percentage of infiltrating T helper cells (gated as CD8$^-$ CD3$^+$, which largely correspond to CD4$^+$ T lymphocytes) in isotype and α-PD-1 antibody-treated mice among hematopoietic cells. F) Percentage of PD-1$^+$, Lag-3$^+$, and 2B4$^+$ among CD8$^+$ T cells infiltrating tumors from isotype-treated *CD4cre Ptpn11$^{fl/fl}$* and *Ptpn11$^{fl/fl}$* mice. Results depict n=7-11 mice/group (C, *right panel*), and mean ± SEM of n=7-8 mice/group (A, *left panel*), of n=9-11 mice/group (B), of n=3-9 mice/group (D-F). Data are a pool of two independent experiments (A-D and F) and a representative graph of two independent experiments (E). Only statistically significant differences are indicated; Student's t-test. C) For survival, comparisons are by log-rank (Mantel-Cox) test.

Supplemental Experimental procedures

Flow cytometry: surface and intracellular staining
For flow cytometry analysis, cells were pre-incubated with α-CD16/32 (2.4G2) to block Fc receptors and then surface stained using antibodies against CD3e (145-2C11), CD4 (GK1.5, RM4-5), CD5 (53-7.3), CD8a (53-6.7), CD24 (M1/69), CD44 (IM7), CD45.1 (A20), CD45.2 (104), CD62L (MEL-14), CD69 (H1.2F3), PD-1 (J43, 29F.1A12), Lag3 (ebioC9B7W), 2B4 (ebio244F4), Tigit (1G9), and CD107 (ebio1D4B). Antibodies were purchased from eBioscience or Biolegend. The H-2Db–gp33 H-2Db–gp276 tetramer was from TCMetrix. Stainings were performed with appropriate combinations of fluorophores; streptavidin conjugated fluorophores were from eBioscience. To gate on thymocytes, the lineage mix used contained anti-B220 (RA3-6B2), -NK1.1 (PK136), -F4/80 (BM8), -CD11c (N418), and -TCRγδ (eBioGL3). Proliferation was assessed by the detection of Ki67 ex vivo. Intracellular staining for Ki67 (anti-Ki67, clone SolA15) was performed post surface staining using the Transcription factor fixation/permeabilization buffer from eBioscience following the recommended protocol. Transcription factors were detected using the transcription factor staining kit from eBioscience and staining with mAbs for Eomes (Dan11mag), T-bet (eBio4B10) (both from eBioscience) or Tcf1 (C63D8, Cell Signaling) followed by anti-rabbit IgG APC (SouthernBiotech). Data were acquired with a Becton Dickinson flow cytometer and analysed using FlowJo software (Tree Star).

Cytokine production/degranulation capacity assay
Total splenocytes from LCMV-infected mice were cultured for two hours with anti-CD3 or anti-CD3/CD28 (coated overnight with 2 μg/ml anti-CD3e (145-2C11-ebio, eBioscience) only, or 2 μg/ml anti-CD3e and 2 μg/ml of anti-CD28 (37.51, eBioscience)). Then, Brefeldin A (10 μg/ml) was added and cells were cultured for two additional hours. For gp33 peptide restimulation, total splenocytes were incubated 4 hours with 1 μM LCMV gp (33-41) peptide (EMC microcollections), in the presence of Brefeldin A (10 μg/ml) for the last 3 hours. Cells were first surface stained, then fixed with 4% paraformadeyde and permeabilized with 0.5% saponin (Sigma) in PBS for 15 minutes. After permeabilization, cells were then stained for the indicated cytokines (TNF-α clone MP6-XT22, IFN-γ clone XMG1.2, IL-2 clone JE6-5H4). Degranulation capacity was determined incubating the cells during the stimulation with anti-CD107 (ebio1D4B).

Immunoblot analysis
Total T cells and $CD8^+$ T cells were enriched using α-CD4 and α-CD8a magnetic beads or α-CD8a magnetic beads (Miltenyi Biotec) only, respectively. T cell purity was over 90%, whereas T cell contamination in T cell-depleted spenocytes less than 5%. Rabbit polyclonal anti-mouse Shp-2 (D50F2) and Shp-1 (C14H6) were obtained from Cell Signaling. α-β-actin was from Abcam.

Quantitative PCR
RNA extraction, retrotranscription to cDNA, and expression analysis were done as previously described (Ludigs et al., 2015). The Following primers were used:

Ptpn11 fwd: 5'- AGACTTCGTTCTCTCCGTGC-3'
Ptpn11 rev 5'- CTGTCAGAGAGTCAAAGCGC-3'

polr2a fwd 5'- CCGGATGAATTGAAGCGGATGT-3'
polr2a rev: 5'-CCTGCCGTGGATCCATTAGTCC-3'

Supplemental References
Grossmann, K.S., Wende, H., Paul, F.E., Cheret, C., Garratt, A.N., Zurborg, S., Feinberg, K., Besser, D., Schulz, H., Peles, E., et al. (2009). The tyrosine phosphatase Shp2 (PTPN11) directs Neuregulin-1/ErbB signaling throughout Schwann cell development. Proceedings of the National Academy of Sciences of the United States of America 106, 16704-16709.
Ludigs, K., Seguin-Estevez, Q., Lemeille, S., Ferrero, I., Rota, G., Chelbi, S., Mattmann, C., MacDonald, H.R., Reith, W., and Guarda, G. (2015). NLRC5 Exclusively Transactivates MHC Class I and Related Genes through a Distinctive SXY Module. PLoS genetics 11, e1005088.
Nishimura, H., Minato, N., Nakano, T., and Honjo, T. (1998). Immunological studies on PD-1 deficient mice: implication of PD-1 as a negative regulator for B cell responses. International immunology 10, 1563-1572.
Pircher, H., Moskophidis, D., Rohrer, U., Burki, K., Hengartner, H., and Zinkernagel, R.M. (1990). Viral escape by selection of cytotoxic T cell-resistant virus variants in vivo. Nature 346, 629-633.